IngentaConnect

Plume Formation During Laser Heating of a Solid Surface

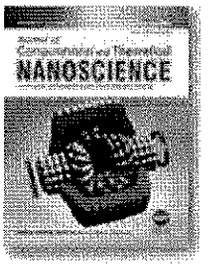

Authors: Kim, Kwang Ryul; Kim, Jae-Hoon; Kang, Namhyun; Cho, Sung Hak; Kim, Kwang Ho

Source: Journal of Computational and Theoretical Nanoscience, Volume 5, Number 8, August 2008 , pp. 1592-1596(5)

Publisher: American Scientific Publishers

< previous article | next article > | view table of contents

Abstract:

A mathematical model of the dynamics of laser-produced heating, evaporation and plume formation is presented. The condensed material model includes conduction heat transfer as well as melting and evaporation phase changes. The localized heating and evaporation caused by focused laser radiation forms a plume of mixed vapor above the material surface. The beam is absorbed and refracted as it traverses the plume, thus modifying its power density on the surface. In this work, variations of heat transfer rate during laser heating and effects of a plume formed by vapor from an iron surface are studied using an axisymmetric mass, momentum and energy transport model. The simulation results quantify the heat transfer rate in the plasma plume, heat losses due to radiation, and variations of heat input into the material.

References: 8 references open in new window

Articles that cite this article?

Keywords: LASER-PRODUCED PLASMA PLUME; LASER-MATTER INTERACTION; PLUME DYNAMICS

Document Type: Research article

DOI: 10.1166/jctn.2008.831

Journal of
Computational and Theoretical Nanoscience
Vol. 5, 1–5, 2008

Plume Formation During Laser Heating of a Solid Surface

Kwang Ryul Kim[1,*], Namhyun Kang[2], Sung Hak Cho[3], and Kwang Ho Kim[1]

[1] National Core Research Center for Hybrid Materials Solution, Pusan National University, Busan 609-735, South Korea
[2] Department of Materials Science and Engineering, Pusan National University, Busan 609-735, South Korea
[3] KIMM (Korea Institute of Machinery and Materials), 171 Jang-dong, Yuseong-Gu, Daejeon 305-343, South Korea

A mathematical model of the dynamics of laser-produced heating, evaporation and plume formation is presented. The condensed material model includes conduction heat transfer as well as melting and evaporation phase changes. The localized heating and evaporation caused by focused laser radiation forms a plume of mixed vapor above the material surface. The beam is absorbed and refracted as it traverses the plume, thus modifying its power density on the surface. In this work, variations of heat transfer rate during laser heating and effects of a plume formed by vapor from an iron surface are studied using an axisymmetric mass, momentum and energy transport model. The simulation results quantify the heat transfer rate in the plasma plume, heat losses due to radiation, and variations of heat input into the material.

Keywords: Laser-Produced Plasma Plume, Laser-Matter Interaction, Plume Dynamics.

RESEARCH ARTICLE

1. INTRODUCTION

When a continuous-wave (CW) laser beam is focused on the material surface, a portion of laser energy is absorbed into the material. This high energy density causes localized heating and evaporation. Optimization of laser materials processing involves determining a set of process parameters that leads to stable processing conditions. Since accurate laser joining experimental data for improving the process and decreasing defects is limited, numerous researchers have studied theoretical and numerical models for laser-produced melting and evaporation.

Some researchers developed mathematical models to calculate the heat flow and motion of molten metal inside the keyhole.[1–7] As a result of melting and evaporation, a plume of hot, ionized material vapor mixed with ambient gas forms above the surface. An example of a process where plume formation is important is CO_2 laser welding.[8] Experimental measurements show that the material vapor/ambient gas mixture which form at irradiances for typical of welding is partially ionized.[9–10] However, these gases absorb infrared wavelength by the inverse Bremsstrahung mechanism and electron density gradients refract the beam so as to defocus it.[11] Hence, the power and trajectory of the laser beam are modified as it traverses the plume and the laser power density impinging on the material surface is decreased as the plume-beam interaction effects become stronger. The coupled dynamic model of the plume and beam propagation is used to calculate the dynamic beam radius and intensity changes on the material surface during CO_2 laser-material interaction.

2. LASER-PRODUCED EVAPORATION AND PLASMA PLUME MODEL

To model evaporation, one must consider heating of the surface (liquid in this case) and substrate. Assuming constant thermal properties for each phase, the heat conduction in the liquid and solid iron is written in axisymmetric coordinates as

$$\frac{1}{\alpha_p}\frac{\partial T}{\partial t} = \frac{1}{r}\frac{\partial T}{\partial r} + \frac{\partial^2 T}{\partial r^2} + \frac{\partial^2 T}{\partial z^2} \quad (1)$$

The evaporation phase change is represented with Stefan and kinetic boundary equations[13–14] and related nomenclature are well stated in previous paper.[14] As described

*Author to whom correspondence should be addressed.

below, the laser intensity on the material surface is calculated by modeling the propagation of a Gaussian laser beam through the plume. All the required calculations for boundary conditions and material properties are well described in previous paper.[14]

Flow in the plume is induced by evaporation from the material surface. The flow and mixing of the gas/vapor mixture in the plume is modeled with mass, momentum and energy transport equations. In an axisymmetric cylindrical coordinate system, these can be written as[15]

$$\frac{\partial \rho_s}{\partial t}+\frac{1}{r}\frac{\partial}{\partial r}(\rho_s r u_r)+\frac{\partial}{\partial z}(\rho_s u_z)=0 \quad (2)$$

$$\frac{\partial}{\partial t}(\rho u_r)+\frac{1}{r}\frac{\partial}{\partial r}(\rho r u_r^2)+\frac{\partial}{\partial z}(\rho u_r u_z)+\frac{\partial p}{\partial r}-\frac{1}{r}\frac{\partial}{\partial r}(r\tau_{rr})+\frac{\tau_{\theta\theta}}{r}-\frac{\partial}{\partial z}(\tau_{rz})=0 \quad (3)$$

$$\frac{\partial}{\partial t}(\rho u_z)+\frac{1}{r}\frac{\partial}{\partial r}(\rho r u_r u_z)+\frac{\partial}{\partial z}(\rho u_z^2)+\frac{\partial p}{\partial z}-\frac{1}{r}\frac{\partial}{\partial r}(r\tau_{rz})-\frac{\partial}{\partial z}(\tau_{zz})+\rho g=0 \quad (4)$$

$$\frac{\partial E_t}{\partial t}+\frac{1}{r}\frac{\partial}{\partial r}(r u_r E_t)+\frac{\partial}{\partial z}(u_z E_t)+\frac{\partial}{\partial r}(p u_r)+\frac{\partial}{\partial z}(p u_z)+\frac{1}{r}\frac{\partial}{\partial r}(r q_r)+\frac{\partial}{\partial z}(q_z)-\frac{1}{r}\frac{\partial}{\partial r}(r u_r \tau_{rr}+r u_z \tau_{rz})-\frac{\partial}{\partial z}(u_r \tau_{rz}+u_z \tau_{zz})+\frac{u_r}{r}(\tau_{\theta\theta})-\sum \alpha I=0 \quad (5)$$

All the required calculation information for boundary conditions and material properties are well described in previous paper.[14]

When the electric field $E(r, z)$ of a propagating axisymmetric laser beam is written as

$$E(r,z)=U(r,z)\exp(-ikz) \quad (6)$$

it can be shown that the complex scalar amplitude $U(r, z)$ satisfies the paraxial wave equation (Ref. [16])

$$\frac{\partial U(r,z)}{\partial z}=-\frac{i}{2k}\left[\frac{\partial^2}{\partial r^2}+\frac{1}{r}\frac{\partial}{\partial r}+k_{opt}^2(\hat{n}^2-1)\right]U(r,z) \quad (7)$$

The all detailed information for the Eqs. (6) and (7) is in Ref. [20]. The expression for the electron-ion inverse Bremstrahlung absorption coefficient for CO_2 laser radiation assumes partial ionization.[8]

The axisymmetric boundary conditions for the plume simulation are illustrated in Figure 1. All physical and flow properties at the plume simulation inlet are updated at each simulation time step and vary in response to beam absorption at the material surface. To include shielding gas effects, uniform axisymmetric flow of helium or argon gas (10 m/sec) is imposed at the side boundary. It is assumed that the beam absorption into the molten iron is 13%.[7]

To correspond to CW laser interaction, established initial plume velocity and temperature field are assumed.

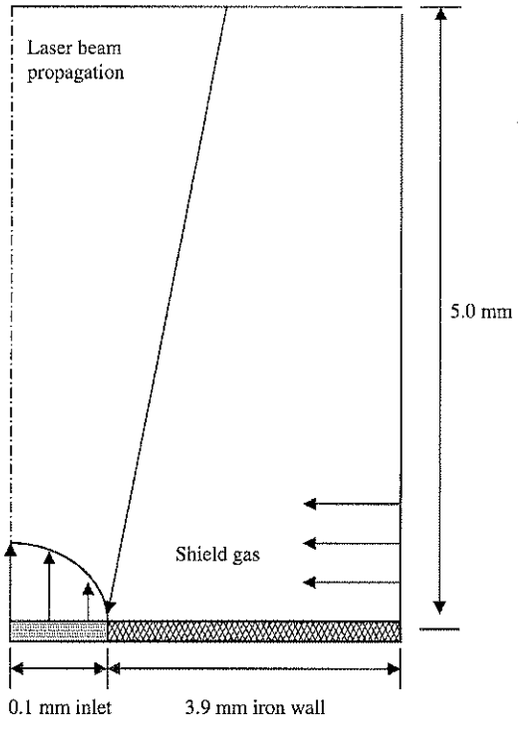

Fig. 1. Physical domain for plume simulation.

The initial plasma plume (which is very small relative to its developed size) is assumed to be elliptical and having Gaussian temperature and velocity distributions. The explicit MacCormack scheme is used to calculate velocity, density and temperature profiles in the plume. The optimal time step is calculated as the minimum of the Von Neumann and Courant-Friedrichs-Levy (CFL) stability conditions. The shield gas and iron vapor mixing is computed using strong coupling of the single-species continuity equations at each time step. The continuity

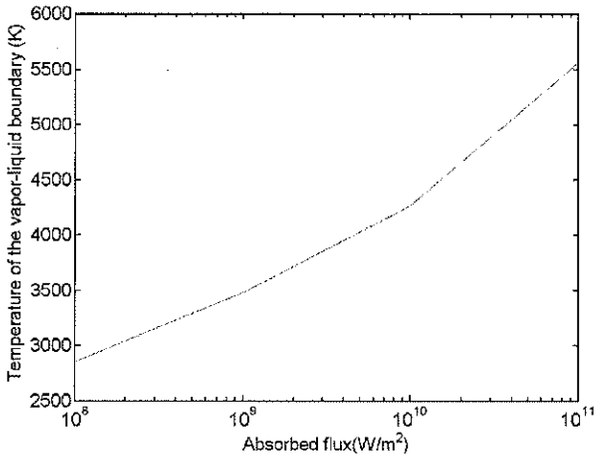

Fig. 2. Steady-state maximum surface temperature as a function of absorbed laser intensity.

equations are combined with the Navier-Stokes equations and computed at the same time step. Boundary conditions for the beam propagation calculation correspond to a collimated 2 cm diameter CO_2 laser beam focused by a 12 cm lens. The laser beam quality is taken as $M^2 = 5$. $U(r, z)$ is calculated where the beam exits the lens and is propagated to the top of the simulation domain by matrix optics.

3. RESULTS OF NUMERICAL STUDY

A plot of simulation results at nominal conditions (3 kW power, 0.1 mm spot radius, 9×10^{10} W m^{-2} surface intensity, helium shielding) are shown in Figure 3. Beginning from the initial conditions, the vapor plasma continuously expanded as a result of the beam absorption. At 2×10^{-5} s after the start, the maximum temperature in the core of the plume reached 8100 K. The plume height is less than 3 mm, the maximum pressure is 37 Patm. and the maximum flow velocity is approximately 900 m s^{-1}. At 3×10^{-5} s, the plume height has increased to over 3 mm. A very small (approx. 0.1 mm thick) high pressure region is sustained near the material surface. It is found that the helium shield plume is stabilized after 3×10^{-5} s from the longer time simulation results. The shielding gas is recognized as a very important parameter in laser materials processing, where helium and argon are both popular options. The plume conditions resulting from laser material interaction under argon shielding gas are presented in Figure 4. The maximum (11,000 K) and average plume temperatures for argon shielding are higher than those predicted for helium shielding. This result corresponds well to experimental measurements made during welding at comparable

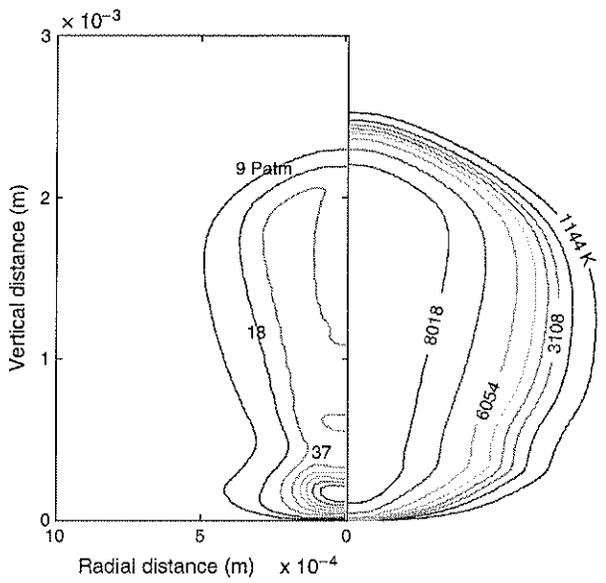

Fig. 3. Pressure contours (Patm) and temperatures (K) at 2×10^{-5} s, helium shield gas.

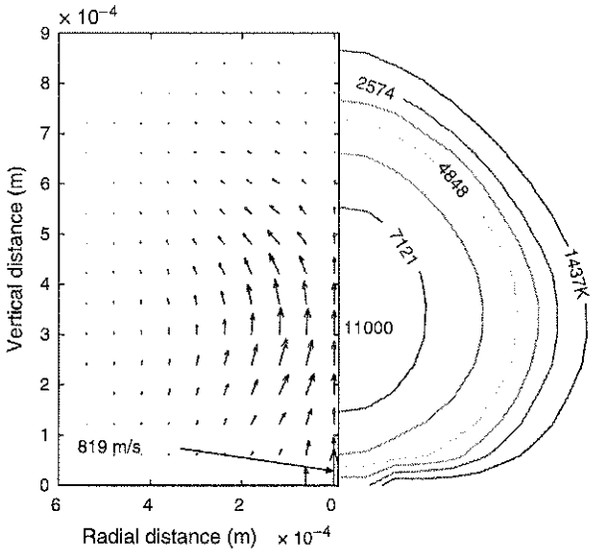

Fig. 4. Velocity (m s^{-1}) and temperature (K) profiles at 5×10^{-6} s, argon shield gas.

powers, where maximum plume temperatures from 9000 K to 13,000 K (Ref. [10]) have been reported.

The predicted variation of the index of refraction and the absorption coefficient within the plume are shown in Figure 5 for helium shielding gas. The index of refraction decreases from 1.0 in the un-ionized gas/vapor outside the plume to 0.995 near its core. The absorption coefficient increases from 0 to 42 m^{-1}. For argon case, the

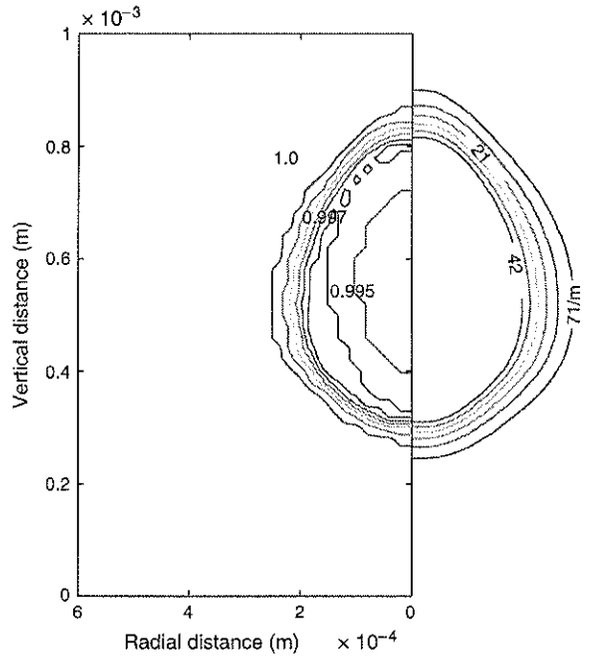

Fig. 5. Real part of index of refraction and absorption coefficients (m^{-1}) at 5×10^{-6} s, helium shield gas.

RESEARCH ARTICLE

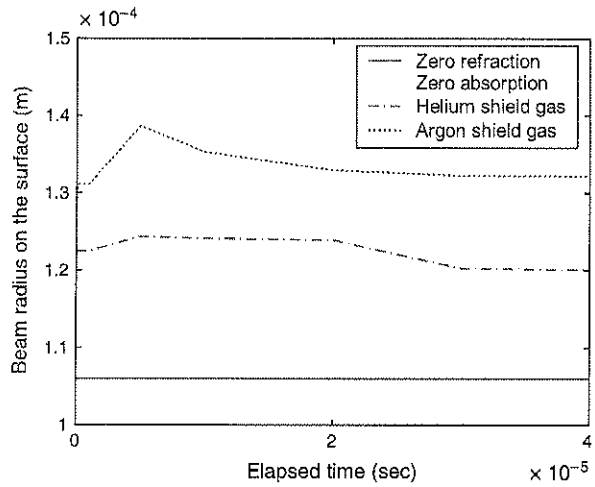

Fig. 6. Beam radius changes at the material surface for various plume interaction conditions and shielding gases.

absorption coefficient increases from 0 to 103 m^{-1}. The beam radius variations with vertical distance for the two different shielding gases are presented in Figure 6. The radius increase is more pronounced for the argon plume, due to its larger index of refraction gradient. The beam radius changes on the material surface are quantified in Figure 6, at simulation times up to 4×10^{-5} s. The beam radius for the helium shield case is about 15% larger than the un-refracted case and remains fairly steady over the time interval. The beam radius for argon shielding increased rapidly by about 20% then grew to 33% but was decreasing somewhat at the end of the simulation time. The zero refraction and zero absorption cases are discussed in more detail below.

The beam irradiance changes on the material surface for helium and argon shielding are shown in Figure 7.

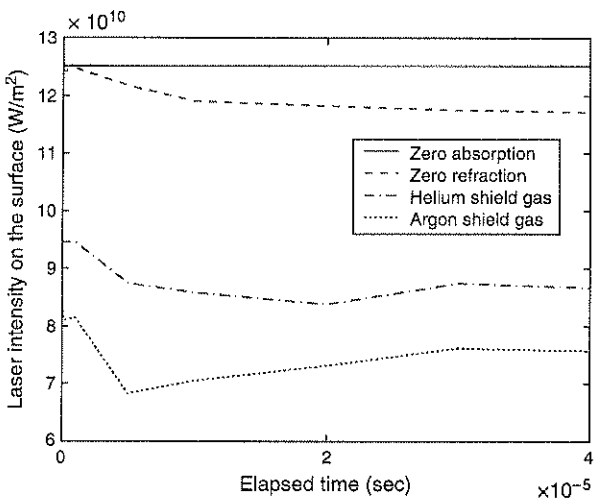

Fig. 7. Time variation of beam irradiance adjacent the material surface for various plume interaction and ambient atmosphere conditions.

These curves correspond very closely to the focal spot radius changes in Figure 6, indicating that power density on the material surface is decreased by defocusing and absorption. Over the simulation time, the beam intensity decreased by 26% for helium shielding gas and by 46% for argon shielding gas. When absorption was included in the plume simulation but refraction was not, the plume was fully formed, but the beam intensity at the material surface was only reduced by 3%. Thus, the significant power density decreases predicted by the lower two curves in Figure 7 are mostly due to refraction. Considering the combined effects of beam radius and intensity changes for helium shield gas case at steady state (4×10^{-5} s), we found that the heat transfer rate into material is 511 W and decreased by 11% comparing with zero absorption case. Heat transfer rate in the helium-iron vapor is calculated by mass and energy balance equations (Ref. [17]) at steady state. Based on 3000 W input powers, we obtained 663 W for energy absorption and re-absorption in the vapor plume and 11 W for energy loss due to radiation.

4. CONCLUSIONS

An axisymmetric heat transfer model of the plasma plume formed by a CO_2 laser beam impinging on a flat iron surface has been described. The following conclusions are drawn from the simulation results.

The CO_2 laser beam is significantly defocused as it propagates through the plasma plume. Refraction of the propagating CO_2 laser beam in the plasma plume has a much larger direct effect on the beam power density at the material surface than absorption does. However, without absorption, the plume quickly dissipates. Thus, indirectly, the plume absorption also has a large impact on power density at the material surface. Less beam refraction and absorption are observed for helium shielding gas than argon. Surface power density changes that calculated as the plume evolves have non-trivial effects on the properties of the metal vapor entering the plume. Laser energy reflected from the material surface has significant effects on plume properties and stability. For the helium shield CO_2 laser welding, heat transfer rate into material is decreased by 11% due to absorption and refraction effects.

Acknowledgments: This work was supported by a grant from the National Core Research Center (NCRC) Program funded by KOSEF and MOST (R15-2006-022-01001-0).

References

1. J. Dowden, M. Davis, and P. Kapadia, *J. Appl. Phys.* 57, 4474 (1985).
2. F. K. Chung and P. S. Wei, *ASME Journal of Heat transfer* 121, 451 (1999).
3. M. F. Modest, *ASME Journal of Heat Transfer* 118, 774 (1996).

4. M. F. Modest and H. Abakians, *ASME Journal of Heat Transfer* 108, 602 (**1986**).
5. A. Kaplan, *J. Phys. D: Appl. Phys.* 27, 18051 (**1994**).
6. A. Kar and J. Mazumder, *J. Appl. Phys.* 78, 6353 (**1995**).
7. J. Xie and A. Kar, *J. Appl. Phys.* 81, 3015 (**1997**).
8. W. W. Duley, Laser Welding, John Wiley & Sons, Inc., New York (**1998**).
9. A. Poueyo-Verwaerde, R. Fabbro, G. Deshors, A. M. de Frutos, and J. M. Orza, *J. Appl. phys.* 74, 5773 (**1993**).
10. Z. Szymanski and J. Kurzyna, *J. Appl. Phys.* 76, 7750 (**1993**).
11. T. P. Hughes, Plasmas and Laser Light, John Wiley & Sons, Inc., New York (**1975**).
12. E. Sobol, Phase Transformations and Ablation in Laser-Treated Solids, John Wiley and Sons, New York (**1995**).
13. M. V. Allmen and A. Blatter, Laser-Beam Interactions with Materials, Springer-Verlag, Berlin Heidelberg (**1995**).
14. K. R. Kim and D. F. Farson, *J. Appl. Phys.* 89, 681 (**2001**).
15. K. A. Hoffmann and S. T. Chiang, Computational Fluid Dynamics Vols I, II, Engineering Education System, Wichita, KS (**1998**).
16. B. E. A. Saleh and M. C. Teich, Fundamentals of Photonics, John Wiley and Sons, New York (**1991**).
17. S. Sankaranarayanan and A. Kar, *J. Phys. D: Appl. Phys.* 32, 777 (**1999**).

Received: 8 July 2007. Accepted: 15 October 2007.